SUPPORTING MATERIAL

MEMBRANE-PROXIMAL EXTERNAL HIV-1 gp41 MOTIF ADAPTED FOR DESTABILIZING THE HIGHLY RIGID VIRAL ENVELOPE

Beatriz Apellániz, Andrey Ivankin, Shlomo Nir, David Gidalevitz, and José L. Nieva

Materials and Methods

Materials

The MPER-derived KKKNWFDITNWLWYIKLFIMIVGGLVKK (CpreTM) and NEQELLELDKWASLWNWFNITNWLWYIK (MPERp) peptides used in this study were produced by solid-phase synthesis using Fmoc chemistry as C-terminal carboxamides and purified by HPLC. 1-palmitoyl-2-oleoyl-sn-glycero-3-phophocholine (POPC), 1,2-dipalmitoyl-sn-glycero-3-phophocholine (DPPC), 1-stearoyl-2-hydroxy-sn-glycero-3-phosphocholine (LPC), 1,2-dioleoyl-sn-glycerol (DG) and Cholesterol (Chol) were purchased from Avanti Polar Lipids (Birmingham, AL, USA). The 8-aminonaphtalene-1,3,6-trisulfonic acid sodium salt (ANTS) and p-xylenebis(pyridinium)bromide (DPX) were obtained from Molecular Probes (Junction City, OR, USA).

Lipid vesicle assays

Large unilamellar vesicles (LUVs) were prepared according to the extrusion method in 5 mM Hepes, 100 mM NaCl (pH 7.4) using membranes with a nominal pore-size of 0.1 μm. Distribution of sizes, estimated by quasielastic light scattering using a Malvern Zeta-Sizer Nano ZS instrument (Malvern Instruments, Malvern, UK), revealed mean diameters ranging between of 110 and 120 nm for the vesicles used in the experiments. The vesicle size distribution did not significantly change upon the addition of peptides at the highest tested doses (i.e., 1:100 peptide-to-lipid ratio). Chol content in vesicles was determined after extrusion by the cholesterol oxidase/peroxidase method (BioSystems, Barcelona, Spain) and found to be within the experimental error.

Peptide incorporation into membranes under our experimental conditions was evaluated by monitoring the change in the emitted Trp-fluorescence (Fig. S1). The apparent mole fraction partition coefficients, $K_{X(app)}$, were determined as described in (White, S. H., W. C. Wimley, A. S. Ladokhin, and K. Hristova. 1998. Protein folding in membranes: determining energetics of peptide-bilayer interactions. Methods Enzymol 295:62-87). Partitioning curves were estimated from the fractional change in Trp fluorescence with increasing lipid concentrations. The peptide concentration was 0.5 μM. The experimental values were fitted to hyperbolic functions (Fig. 2, right panels):

$$F/F_0 = 1 + \frac{[(F_{max}/F_0)-1]\,[L]}{K + [L]}$$

where [L] is the lipid concentration and K is the lipid concentration at which the bound peptide fraction is 0.5. Therefore, $K_{X(app)} = [W]/K$ where [W] is the molar concentration of water.

Vesicle permeabilization was monitored following the release to the medium of encapsulated fluorescent ANTS (ANTS/DPX assay: Ellens, H., J. Bentz, and F. C. Szoka. 1985. H^+- and Ca^{2+}-induced fusion and destabilization of liposomes. Biochemistry 24:3099-3106) and the mechanism (either "graded" or "all-or-none")

established using the "requenching assay" developed by Ladokhin et al. (Ladokhin, A. S., W. C. Wimley, K. Hristova, and S. H. White. 1997. Mechanism of leakage of contents of membrane vesicles determined by fluorescence requenching. Methods Enzymol 278:474-486). In brief, CpreTM was assayed within a range of concentrations allowing final leakage extents below 100 % (see Fig. 5B). The peptide was added to stirring mixtures containing 100 μM lipid vesicles with entrapped ANTS (5 mM) and DPX (8 mM) in 5 mM Hepes. Peptide and vesicles were incubated for 60 min. Then, the decrease in ANTS fluorescence intensity was recorded in each sample upon sequential quenching of ANTS outside vesicles by externally added DPX (25 μl aliquots from a 45 mM stock solution were added 4 times). Subsequently, an excess Triton X-100 (25 μl from a 10% w/v stock) was added to establish the fluorescence intensity corresponding to complete leakage. Fluorescence intensities were finally corrected for dilution. The methodology followed to determine Q_{in} and f_{out} parameters from these ANTS fluorescence values has been detailed by Ladokhin et al. in the above cited paper.

Viral infectivity assays

Pseudoviruses were produced as previously described (Julien, J. P., N. Huarte, R. Maeso, S. G. Taneva, A. Cunningham et al. 2010. Ablation of the complementarity-determining region H3 apex of the anti-HIV-1 broadly neutralizing antibody 2F5 abrogates neutralizing capacity without affecting core epitope binding. J Virol 84:4136-4147) by transfection of human kidney HEK293T cells with the full-length *env* clone pHXB2-env (AIDS Research and Reference Reagent Program, Division of AIDS, NIAID, NIH, contributed by K. Page and D. Littman), or VSV-G encoding pMD2.G plasmid, using calcium phosphate. Each plasmid was co-transfected with vectors pWXLP-GFP and pCMV8.91, encoding respectively a green fluorescent protein and an *env*-deficient HIV-1 genome (kindly provided by Dr. Patricia Villace, CSIC, Madrid). Peptide-induced inhibition was determined using TZM-bl target cells (obtained from the AIDS Research and Reference Reagent Program, Division of AIDS, NIAID, NIH, and contributed by J. Kappes). Neutralization levels after 72 hours were inferred from the reduction in the number of GFP-positive cells as determined by flow cytometry using a BD FACScalibur Flow Cytometer (Becton Dickinson Immunocytometry Systems, Mountain View, CA).

Lipid monolayer assays

Both grazing incidence x-ray diffraction (GIXD) and X-ray reflectivity (XR) are well-established techniques for studying Langmuir monolayers at the air-liquid interface, and their application to the characterization of the interactive properties of membrane lipids and peptides has been described in preceding papers (Gidalevitz, D., Y. Ishitsuka, A. S. Muresan, O. Konovalov, A. J. Waring et al. 2003. Interaction of antimicrobial peptide protegrin with biomembranes. Proc Natl Acad Sci U S A 100:6302-6307; Neville, F., M. Cahuzac, O. Konovalov, Y. Ishitsuka, K. Y. Lee et al. 2006. Lipid headgroup discrimination by antimicrobial peptide LL-37: insight into mechanism of action. Biophys J 90:1275-1287; Neville, F., Y. Ishitsuka, C. S. Hodges, O. Konovalov, A. J. Waring et al. 2008. Protegrin interaction with lipid monolayers: Grazing incidence X-

ray diffraction and X-ray reflectivity study. Soft Matter 4:1665-1674; Ivankin, A., I. Kuzmenko, and D. Gidalevitz. 2010. Cholesterol-phospholipid interactions: new insights from surface x-ray scattering data. Phys Rev Lett 104:108101; Neville, F., A. Ivankin, O. Konovalov, and D. Gidalevitz. 2010. A comparative study on the interactions of SMAP-29 with lipid monolayers. Biochim Biophys Acta 1798:851-860). The methodology followed in this study is described in detail in the captions for Figs. S2 and S3.

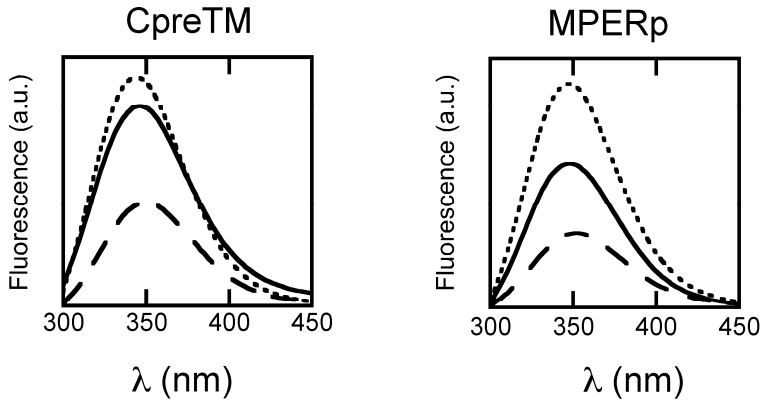

Supplementary Figure 1. Fluorescence emission spectra (excitation wavelength: 280 nm) of the peptides, in solution (slashed) or when incubated in the presence of POPC or POPC:Chol (1:1) LUV (dotted and solid spectra, respectively). Peptide and lipid concentrations were 0.5 and 100 μM, respectively. Corrected spectra were recorded using a FluoroMax-3 (Jobin Ybon, Horiba) with excitation set at 280 nm and 2-nm slits.

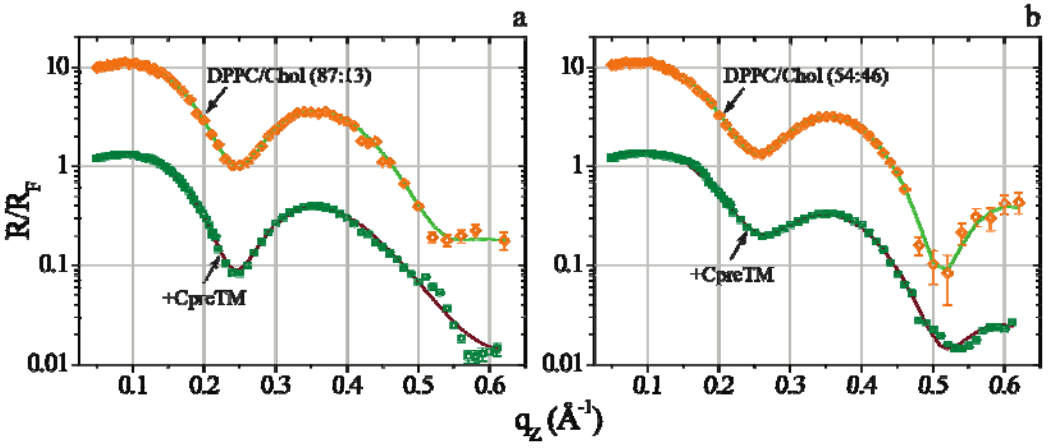

Supplementary Figure 2: X-ray reflectivity data (symbols) and corresponding fits (lines) normalized by Fresnel reflectivity plotted against scattering vector q_Z of (a) DPPC/Chol (87:13) monolayer before (rhombs) and after CpreTM (squares) injection; (b) DPPC/Chol (54:46) monolayer before (rhombs) and after CpreTM (squares) injection. Liquid surface X-ray scattering experiments were performed at the 9-ID beam line at the Advanced Photon Source, Argonne National Laboratory (Argonne, IL). The liquid surface spectrometer (LSS) and Langmuir trough chamber have previously been described (Als-Nielsen, J., D. Jacquemain, K. Kjaer, F. Leveiller, M. Lahav, and L. Leiserowitz. 1994. Principles and applications of grazing-incidence x-ray and neutron-scattering from ordered molecular monolayers at the air-water-interface. Phys Rep 246:252-313.). Langmuir monolayers composed of DPPC/cholesterol with 13 and 46 mol% of cholesterol were used to mimic the virion membrane with depleted and regular content of cholesterol, respectively. Lipid monolayers were formed by depositing droplets of respective solution at the air-liquid interface and after equilibrating for 15 minutes compressed to the surface pressure of 20 mN/m. The peptide solution was then evenly injected underneath the monolayers using a micro-syringe with an L-shaped needle to make up the final concentration of 0.57 μM/L, while the surface pressure was kept constant via proportional-integral-derivative feedback control. Injected peptide interacts with the lipid monolayer and result in an increase in the surface pressure when incorporates into the film. To keep the surface pressure constant, the surface area would have to increase. The resulting relative change in mean molecular area, ΔA/A, was monitored for up to 180 minutes after insertion. The experiments were carried out on Dublecco's phosphate buffered saline without calcium and magnesium (D-PBS) (Invitrogen) at a room temperature of 22 ± 1 °C.

The R&K trough (Riegler & Kirstein GmbH) was sealed in an air-tight canister was flushed with humidified helium for X-ray measurements to reduce X-ray absorption and sample damage. The wavelength of the beam of λ = 0.92017Å was set by a cryogenically cooled Si (111) double-crystal monochromator (Kohzu Seiki Co. Lt.). A split ion chamber monitor and feedback control of the second crystal of the Kohzu monochromator maintained the position of the beam at the monitor (9 m before the sample. Ge (111) steering crystal was used to define the striking angle of the beam onto liquid surface. Incident slits were 2 mm wide and 50 μm high; detector slits were 2x2 mm^2. In reflectivity experiments, scattering intensity is collected as a function of the out-of-plane scattering vector $q_Z = (2\pi/\lambda)\sin\alpha_f$, α_f being the angle of the diffraction beam with the horizontal plane, using a single-channel scintillation detector. XR data were

analyzed using both model-dependent (MD) “slab” model refinement (Neville, F., C. S. Hodges, C. Liu, O. Konovalov, and D. Gidalevitz. 2006. In situ characterization of lipid a interaction with antimicrobial peptides using surface x-ray scattering. Biochim Biophys Acta Biomembr 1758:232-240.; Neville, F., Y. Ishitsuka, C. S. Hodges, O. Konovalov, A. J. Waring, R. Lehrer, K. Y. C. Lee, and D. Gidalevitz. 2008. Protegrin interaction with lipid monolayers: Grazing incidence x-ray diffraction and x-ray reflectivity study. Soft Matter 4:1665-1674) and model-independent (MI) stochastic fitting routines (Danauskas, S. M., D. X. Li, M. Meron, B. H. Lin, and K. Y. C. Lee. 2008. Stochastic fitting of specular x-ray reflectivity data using stochfit. J Appl Cryst 41:1187-1193) employing RFIT2000 (Oleg Konovalov, ESRF) and *StochFit* software, respectively.

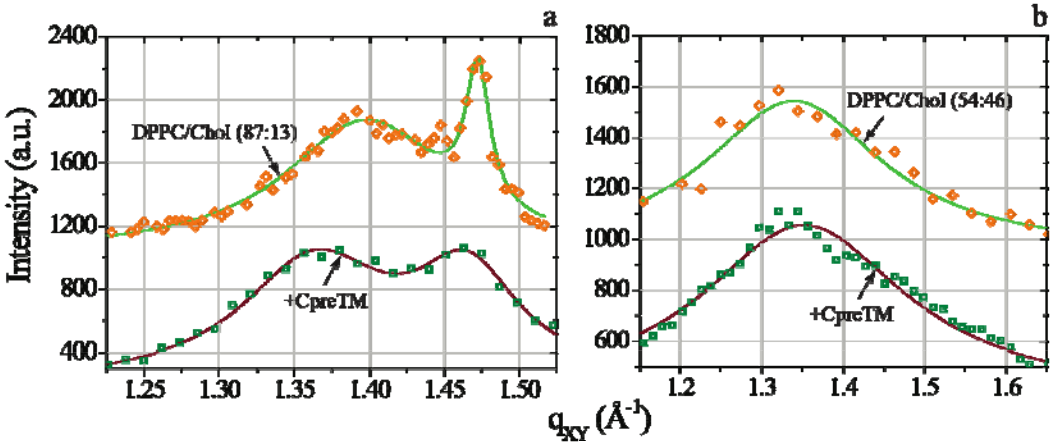

Supplementary Figure 3: Grazing incidence X-ray diffraction data (symbols) and corresponding fits (lines): scattering intensity, integrated over q_Z range, against scattering vector q_{XY} of (a) DPPC/Chol (87:13) monolayer before (rhombs) and after CpreTM (squares) injection; (b) DPPC/Chol (54:46) monolayer before (rhombs) and after CpreTM (squares) injection. To improve sensitivity of X-ray diffraction to the interface, the depth of beam penetration is limited by adjusting the incident angle α_i to $0.85\alpha_c$, with α_c being critical angle for total reflection. A scattering intensity was collected using linear position-sensitive Mythen detector. A scan over a range of q_{xy} integrated over q_z yields Bragg peaks of a 2D periodic structure, whereas the intensity distribution as a function of the out-of-plane scattering vector q_z as at the Bragg peak position q_{xy} is known as a Bragg rod. Several types of information can be extracted from GID measurements. A position of the Bragg peak maximum defines a repeat distance d_{hk} of the 2D lattice structure. The coherence length of the crystallinities can be estimated from the full-width at half-maximum (FWHM) of the Bragg peaks using the Scherrer formula $L = 0.9\times 2\pi/FWHM$ (Patterson, A. L. 1939. The scherrer formula for x-ray particle size determination. Phys Rev 56:978-982). A molecular tilt in the ordered phase is uniquely defined by a position of the Bragg rod maximum.

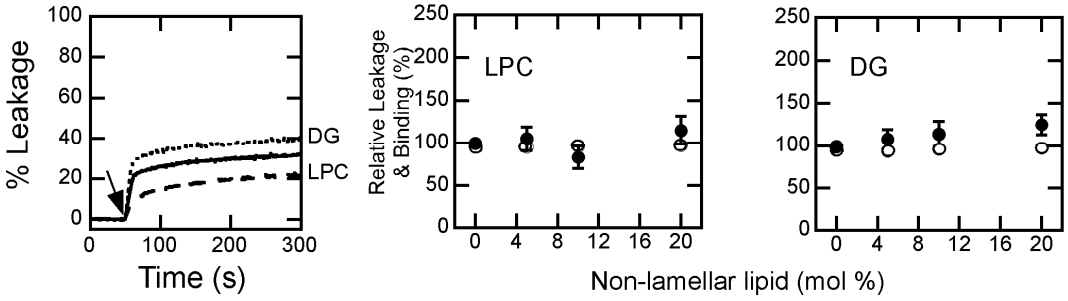

Supplementary Figure 4: Binding to vesicles and final extents of ANTS leakage induced by CpreTM as a function of non-lamellar lipid content. Left: effect of LPC and DG on CpreTM-induced leakage kinetics (dashed and dotted curves, respectively). The peptide was added at the time indicated by the arrow (t = 50 s) at a peptide-to-lipid ratio of 1:400. Non-lamellar lipids were included at 10 mol % in the lipid composition. The solid line corresponds to the control without non-lamellar lipid. Center and Right: Extents of leakage and binding to membranes relative to those measured for vesicles devoid of non-lamellar lipid (black and white circles, respectively). Y axes range as in Fig. 2 (right panels).

Table S1. Summary of CpreTM leakage potencies and qualities of the fits to an "all-or-none" pore model

Chol (mol %)	EC_{50}	EC_{10}[(1)]	R^{2}[(2)]
0	1:300	1:1200	0.9
20	1:1000	1:6000	0.91
33	1:2000	1:13,000	0.96

(1) Effective Peptide-to-lipid mole ratios required to achieve 50 or 10 % of leakage were derived through interpolation of experimental data displayed in Fig. 3A.

(2) Peptide-induced leakage values in Fig. 4B were analyzed according to a mathematical model of "all-or-none" pore formation as previously described (Nicol, F., S. Nir, and F. C. Szoka, Jr. 1996. Effect of cholesterol and charge on pore formation in bilayer vesicles by a pH-sensitive peptide. Biophys J 71:3288-3301). The values in the table denote the qualities of the fittings for octameric CpreTM pores.